

A photograph of a lightning bolt striking a forest silhouette against a dark blue sky. The lightning bolt is bright white and curved, illuminating the surrounding clouds and the dark silhouettes of tall evergreen trees at the bottom.

Towards an Active Target at SPES

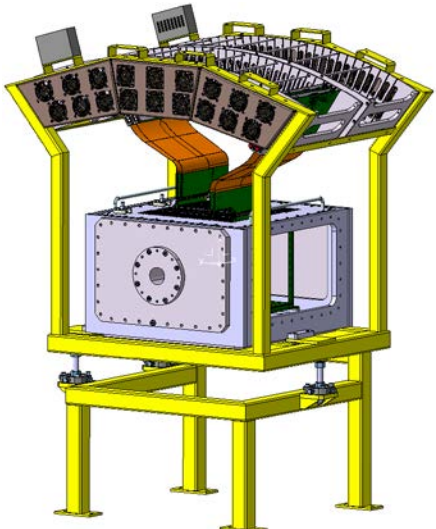
T. Marchi

*Second GDS Topical Meeting
17 Jan 2018
Santiago de Compostela, Spain*

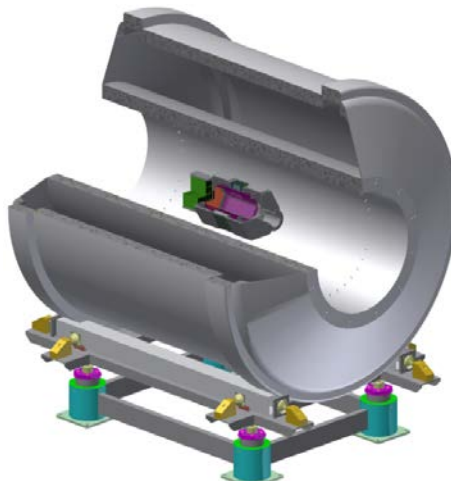
Pan-European activities, ongoing



ACTAR TPC



SpecMAT



Outline

The ATS project and the ACTAR demonstrator

LNS proposal: heavy beams

The SPES facility

Extra: GET/GES + GPUs (?)

ATS



MagicTin^{}*



| | | | | | | | | | | | | | | | | | | | | | | | | | | | | | | | | | | | | | | | | | | | | | | | | | | | | | | | | | | | | | | | | | | | | | | | | | | | | | | | | | | | | | | | | | | | | | | | | | | | |
|---|---|---|---|---|---|---|---|---|----|----|----|----|----|----|----|----|----|----|----|----|----|----|----|----|----|----|----|----|----|----|----|----|----|----|----|----|----|----|----|----|----|----|----|----|----|----|----|----|----|----|----|----|----|----|----|----|----|----|----|----|----|----|----|----|----|----|----|----|----|----|----|----|----|----|----|----|----|----|----|----|----|----|----|----|----|----|----|----|----|----|----|----|----|----|----|----|----|----|-----|
| 1 | 2 | 3 | 4 | 5 | 6 | 7 | 8 | 9 | 10 | 11 | 12 | 13 | 14 | 15 | 16 | 17 | 18 | 19 | 20 | 21 | 22 | 23 | 24 | 25 | 26 | 27 | 28 | 29 | 30 | 31 | 32 | 33 | 34 | 35 | 36 | 37 | 38 | 39 | 40 | 41 | 42 | 43 | 44 | 45 | 46 | 47 | 48 | 49 | 50 | 51 | 52 | 53 | 54 | 55 | 56 | 57 | 58 | 59 | 60 | 61 | 62 | 63 | 64 | 65 | 66 | 67 | 68 | 69 | 70 | 71 | 72 | 73 | 74 | 75 | 76 | 77 | 78 | 79 | 80 | 81 | 82 | 83 | 84 | 85 | 86 | 87 | 88 | 89 | 90 | 91 | 92 | 93 | 94 | 95 | 96 | 97 | 98 | 99 | 100 |
|---|---|---|---|---|---|---|---|---|----|----|----|----|----|----|----|----|----|----|----|----|----|----|----|----|----|----|----|----|----|----|----|----|----|----|----|----|----|----|----|----|----|----|----|----|----|----|----|----|----|----|----|----|----|----|----|----|----|----|----|----|----|----|----|----|----|----|----|----|----|----|----|----|----|----|----|----|----|----|----|----|----|----|----|----|----|----|----|----|----|----|----|----|----|----|----|----|----|----|-----|

$f_{7/2}$ vs $p_{3/2}$ neutron orbitals, in Sn like in Ca?

MagicTin*

| | | | | | | | | | |
|----|---|---|--|--|--|--|------------------|------------------|-------|
| | 134Te 41.8 M | 135Te 19.0 S | 136Te 17.63 S | 137Te 2.49 S | 138Te 1.4 S | 139Te >150 NS | 140Te >300 NS | 141Te >150 NS | 142Te |
| 51 | β^- : 100.00% | β^- : 100.00% | β^- : 100.00% β^-n : 1.31% | β^- : 100.00% β^-n : 2.99% | β^- : 100.00% β^-n : 6.30% | β^-n | β^-n | β^-n | |
| | 133Sb 2.34 M | 134Sb 0.78 S | 135Sb 1.679 S | 136Sb 0.923 S | 137Sb 492 MS | 138Sb 350 MS | 139Sb 93 MS | 140Sb >407 NS | |
| 50 | 132Sn 39.7 S | 133Sn 1.46 S | 134Sn 1.050 S | 135Sn 530 MS | 136Sn 0.25 S | 137Sn 190 MS | 138Sn >408 NS | | |
| | β^- : 100.00% | β^- : 100.00% β^-n : 0.03% | β^- : 100.00% β^-n : 17.00% | β^- : 100.00% β^-n : 21.00% | β^- : 100.00% β^-n : 30.00% | β^- : 100.00% β^-n : 58.00% | β^-n | | |
| 49 | 131In 0.28 S | 132In 0.207 S | 133In 165 MS | 134In 140 MS | 135In 92 MS | | | | |
| | β^- : 100.00% β^-n : 2.00% | β^- : 100.00% β^-n : 6.30% | β^- : 100.00% β^-n : 85.00% | β^- : 100.00% β^-n : 65.00% | β^- : 100.00% β^-n | | | | |
| 48 | 130Cd 162 MS | 131Cd 68 MS | 132Cd 97 MS | 133Cd 57 MS | | | | | |
| | β^- : 100.00% β^-n : 3.50% | β^- : 100.00% β^-n : 3.50% | β^- : 100.00% β^-n : 60.00% | β^- : 100.00% β^-n | | | | | |
| | 82 | 83 | 84 | 85 | 86 | 87 | 88 | | |
| | N=82 | | | | | | | | |

[Adapted from O. Sorlin, M.-G. Porquet,
Progr Part. Nucl Phys 61 (2008) 602]

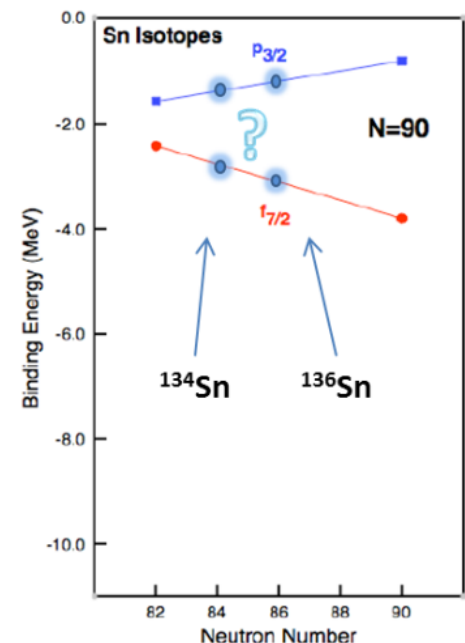
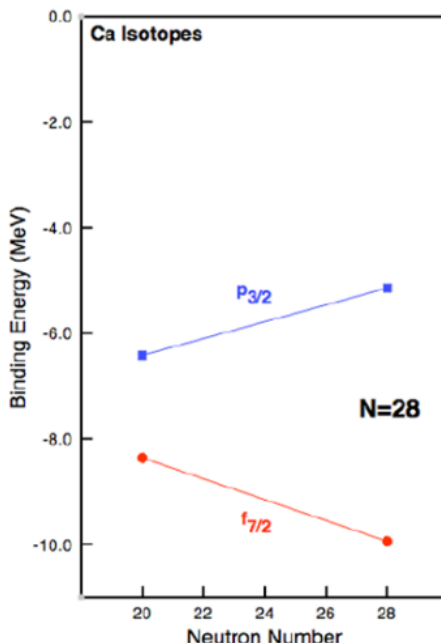


Fig.1 Analogy between $f_{7/2}$ and $p_{3/2}$ evolution of binding energies in the known Ca isotopes to what could be expected for the Sn isotopes approaching $N=90$. Figure adapted from¹³.

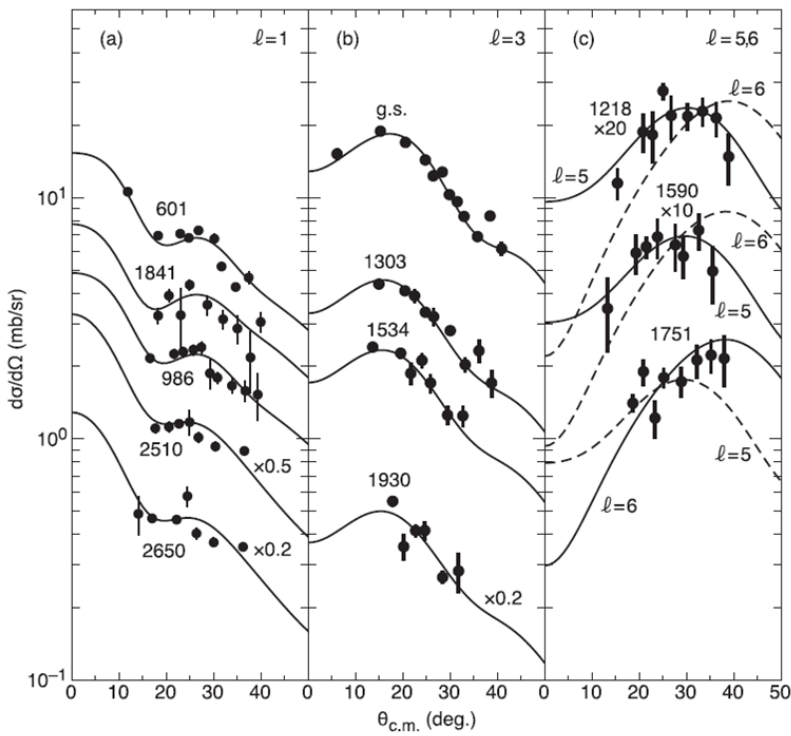
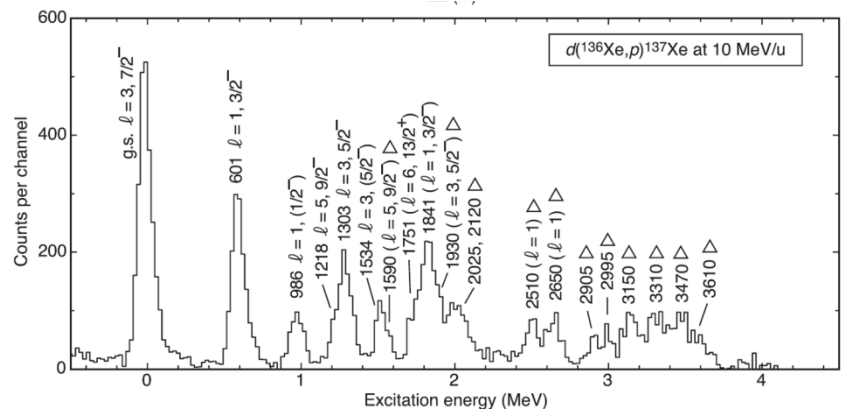
Lol endorsed by SPES SAC

| | SPES 1 st day (5 μ A p beam) | SPES full power (200 μ A p beam) |
|-------|--|---|
| 132Sn | $7.8 \cdot 10^5$ | $3.1 \cdot 10^7$ |
| 133Sn | $7.0 \cdot 10^4$ | $2.8 \cdot 10^6$ |
| 134Sn | $1.2 \cdot 10^4$ | $4.9 \cdot 10^5$ |
| 135Sn | $1.6 \cdot 10^2$ | $6.2 \cdot 10^3$ |
| 136Sn | - | $0.9 \cdot 10^2$ |

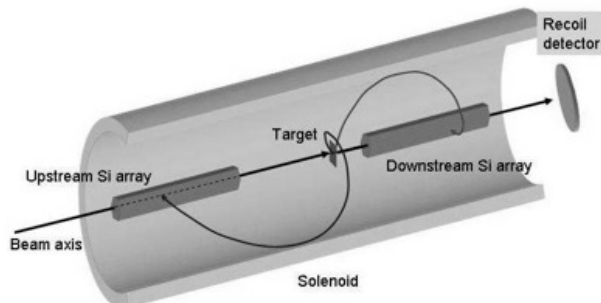
Not only exotic beams

MagicTin*

Reference reaction: $^{136}\text{Xe}(\text{d},\text{p})^{137}\text{Xe}$ - inv kinem



B.P. Kay et al, PRC 84 0243325 (2011)
HELIOS @ ANL



- Possibly extend to $\theta_{\text{cm}} < 10^\circ$
- Study ^{135}I via $(\text{d}, ^3\text{He})$

possible at GANIL or LNS also with high intensity

ACTAR TPC Demonstrator

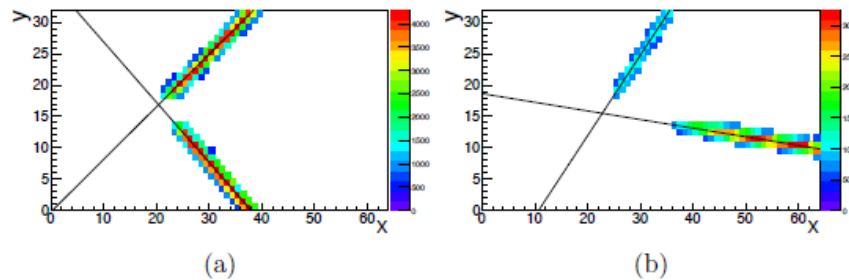
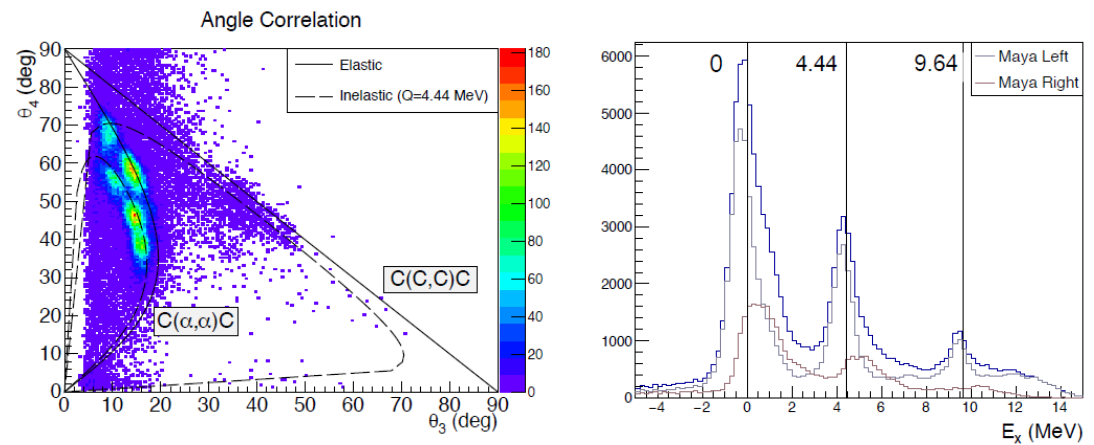
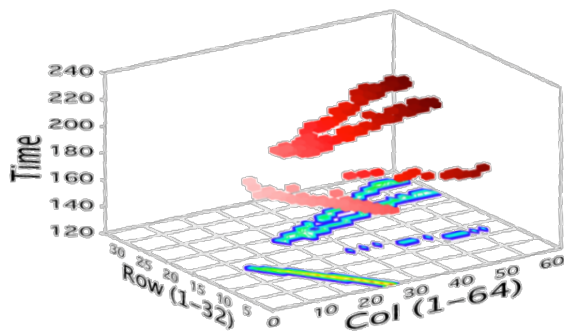
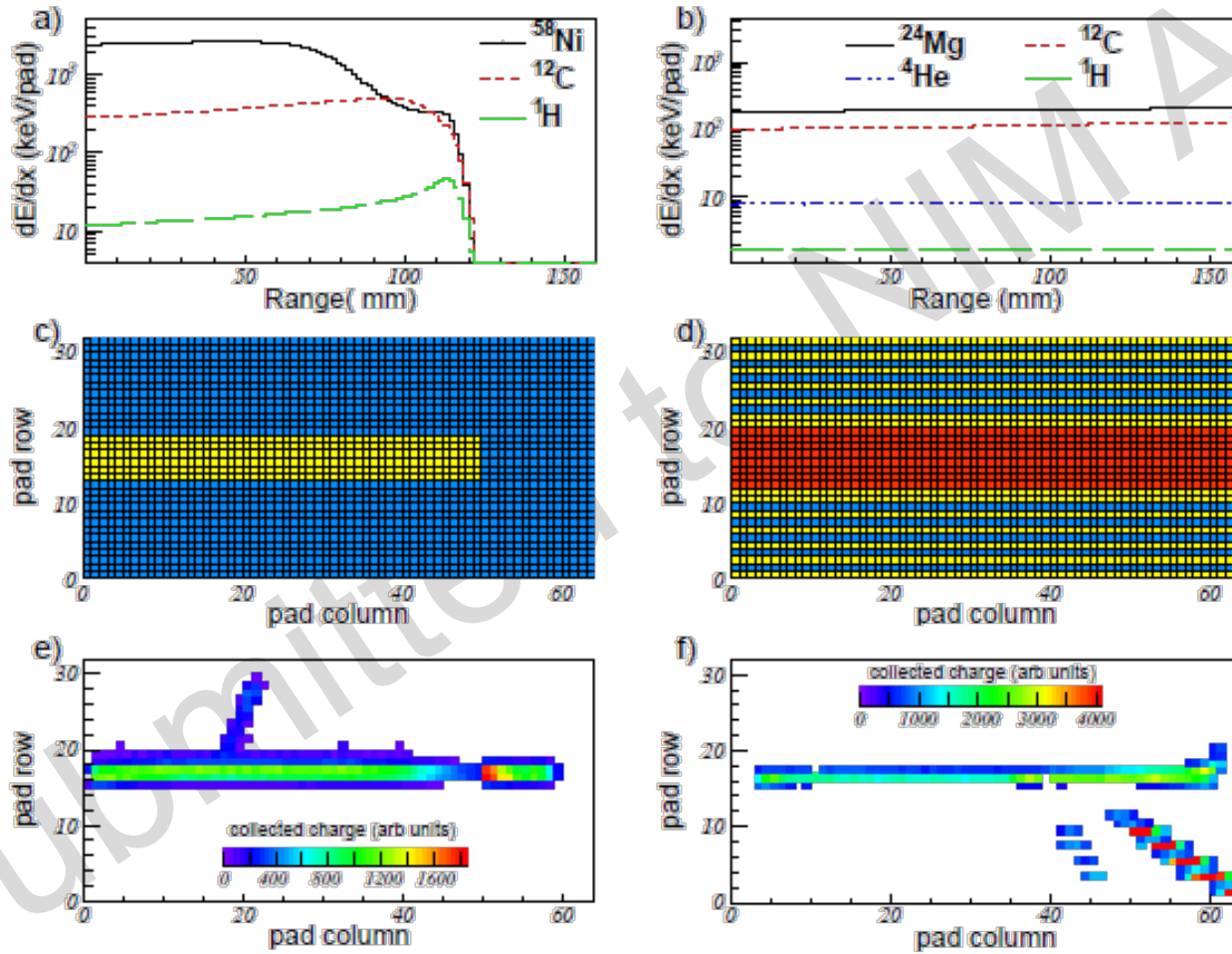


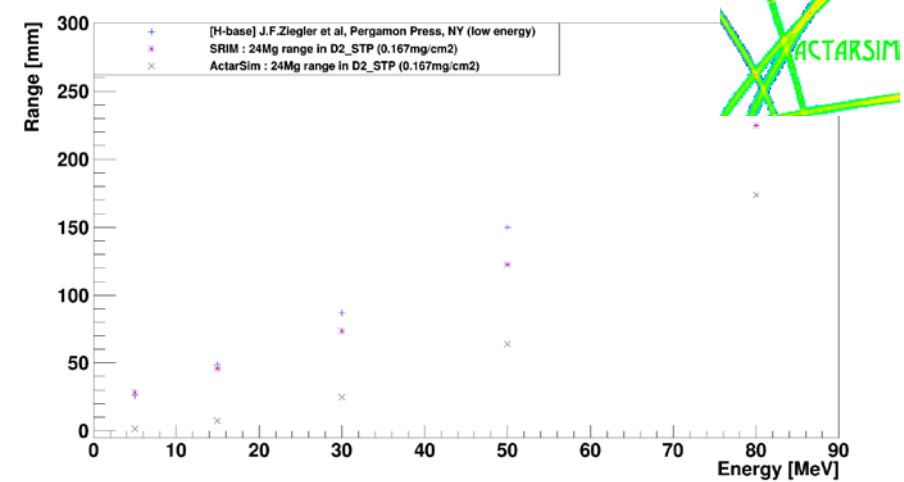
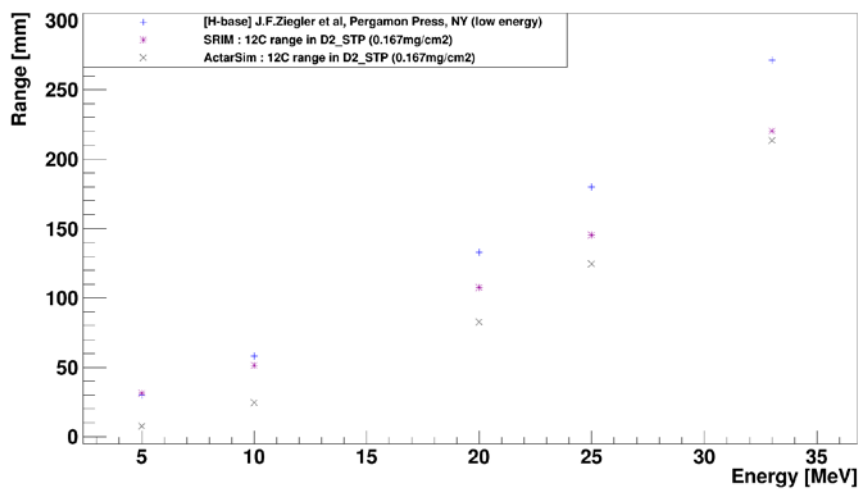
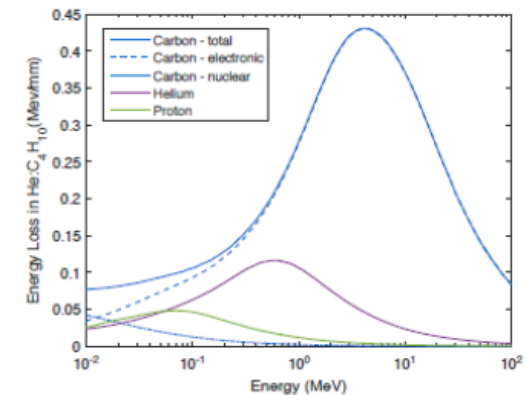
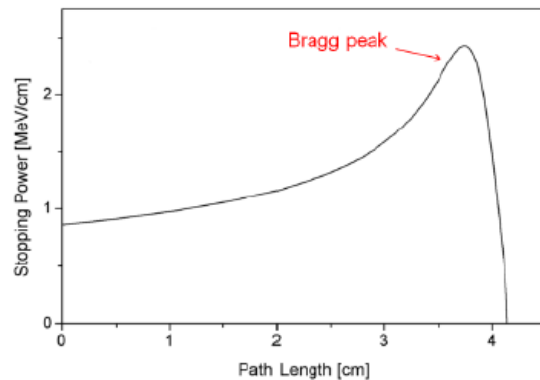
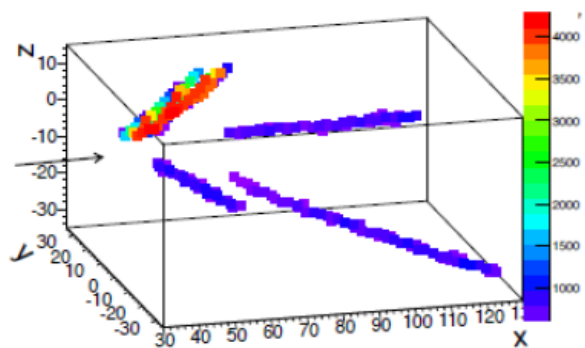
Figure 4.19: Charge deposition on the pad plane of (a) a $^{12}\text{C}(^{12}\text{C},^{12}\text{C})^{12}\text{C}$ and (b) a $^{12}\text{C}(\alpha,\alpha)^{12}\text{C}$ scattering reaction.



ACTAR TPC Demonstrator



Energy loss measurement and calculation



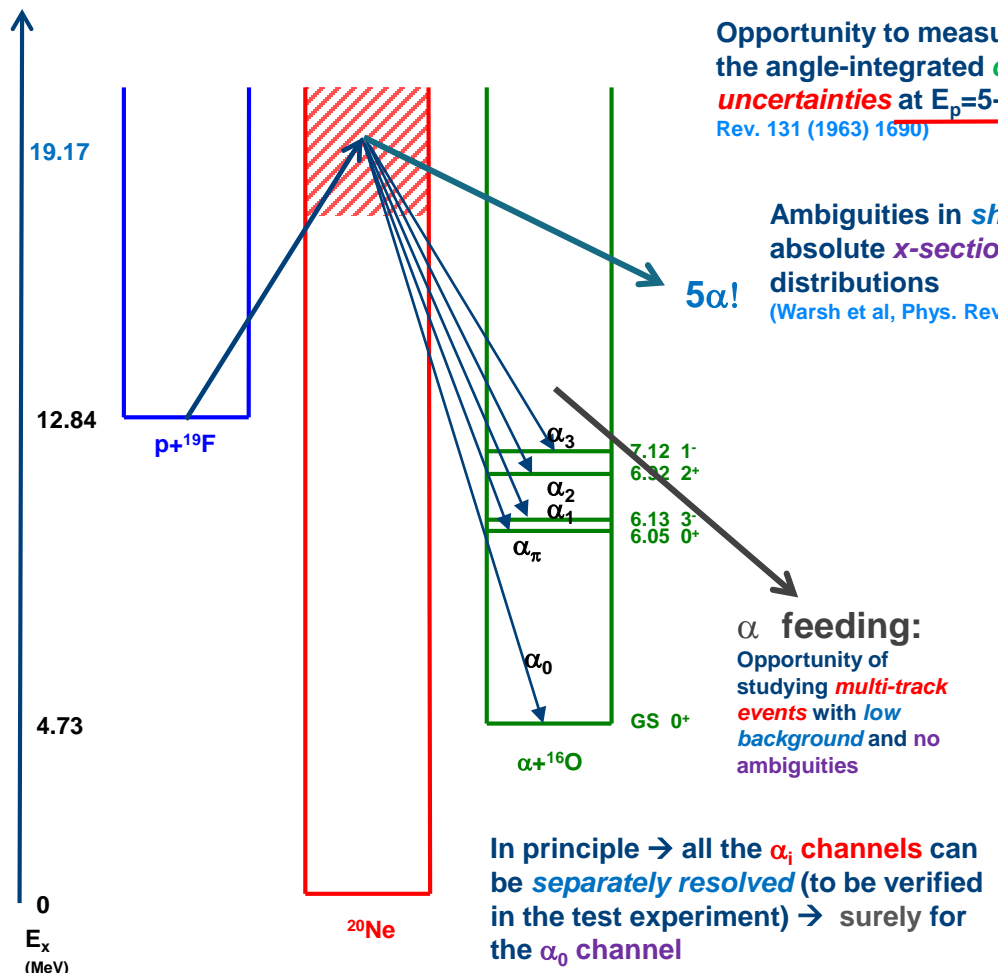
<https://github.com/ActarSimGroup/Actarsim/>

From the LNS proposal

Table 1. List of the proposed projectile for the energy loss profile measurements. As an example, the pressure needed to stop the gas on the pad plane is given for the iC4H10 case.

| Ion | Beam Energy (MeV/u) | Gases to be measured | BTU requested | iC4H10 pressure (mbar) typical case example |
|-------------------|------------------------|--|------------------|--|
| ⁷ Li | 1.0 - 4.5 | H ₂ , D ₂ , CH ₄ , iC ₄ H ₁₀ , CF ₄ , CO ₂ , He | 4.5 | 500 |
| ⁹ Be | 1.5 - 4.5 | | 4.5 | 500 |
| ¹⁰ B | 1.8 - 4.5 | | 4.5 | 500 |
| ¹² C | 2.0 - 4.5 | | 4.5 | 250 |
| ¹⁵ N | 2.0 - 4.5 | | 4.5 | 250 |
| ¹⁶ O | 2.0 - 4.5 | | 4.5 | 250 |
| ¹⁹ F | 2.0 - 4.5 | | 4.5 | 250 |
| ²⁴ Mg | 2.0 - 4.5 | | 4.5 | 250 |
| ⁴⁰ Ca | 2.0 - 3.8 | | 4.5 | 250 |
| ¹²⁰ Sn | 1.5 - 1.7 | | 4.5 | 125 |
| Total | | | 45 | |

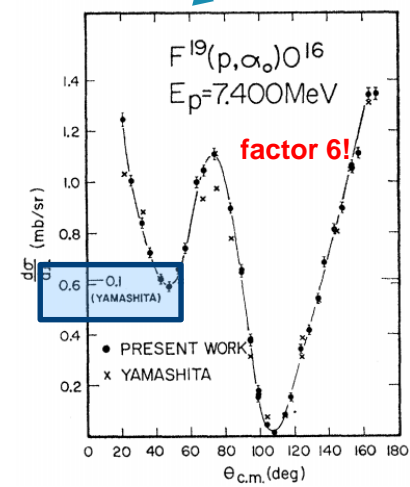
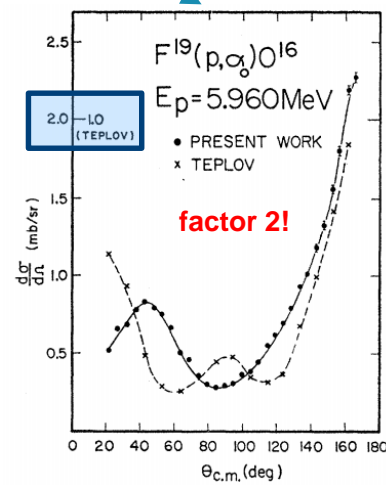
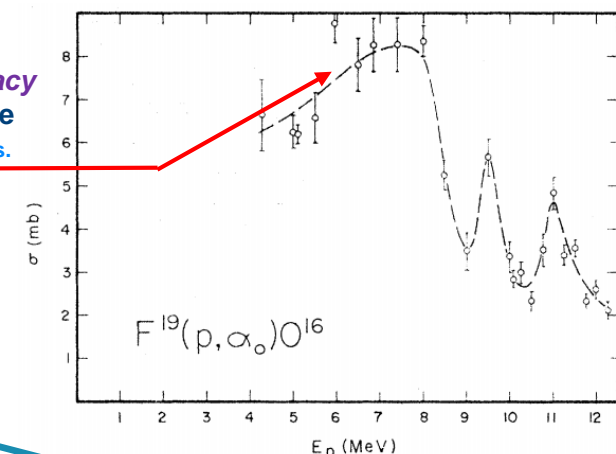
Test case 1: $^{19}\text{F}(\text{p},\text{a})$ reaction at $E_{\text{p}}=5\text{-}7 \text{ MeV}$ (TANDEM)



Opportunity to measure with *good accuracy* the angle-integrated *cross section* → large *uncertainties* at $E_{\text{p}}=5\text{-}7 \text{ MeV}$ (Warsh et al, Phys. Rev. 131 (1963) 1690)

5 α !
Ambiguities in *shapes* and in the absolute *x-section scale* of angular distributions
(Warsh et al, Phys. Rev. 131 (1963) 1690)

α feeding:
Opportunity of studying *multi-track events* with *low background* and *no ambiguities*



Test case 2: $^{120}\text{Sn}(\text{d},\text{p})$ reaction at $E_{\text{Sn}} = 15 \text{ AMeV}$ (CS)

Schneid et al, Phys Rev 156 (1967) 4

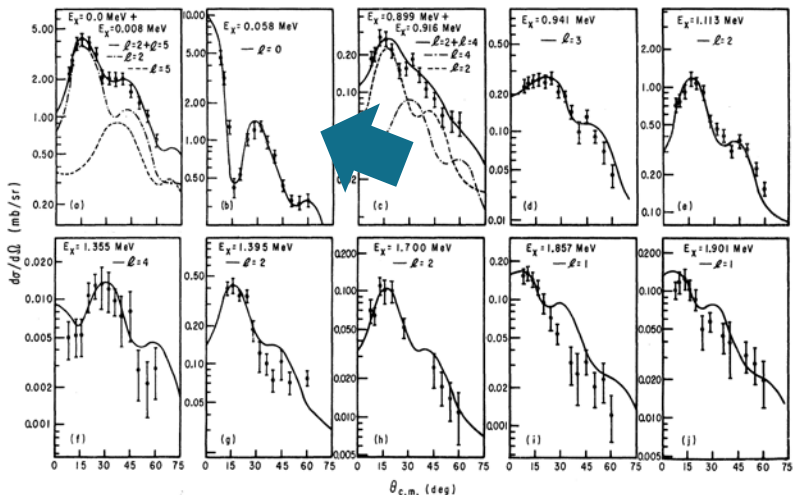


FIG. 2. Angular distributions of transitions in the $^{120}\text{Sn}(\text{d},\text{p})^{121}\text{Sn}$ reaction. The experimental points are given with error bars corresponding to statistics and background subtraction. The solid lines are DWBA curves fitted to the experimental data.

TABLE V. Energy levels of Sn^{121} from the (d,p) and (d,t) reactions.
(See also caption to Table I.)

| E^* (MeV) | I_n | (d,β) J^π | $(d\sigma/d\Omega)_{\text{max}}$ (mb/sr) | $S_{d,p}$ | E^* (MeV) | (d,t) $d\sigma/d\Omega(45^\circ)$ (mb/sr) |
|----------------|-------|------------------------|---|-----------|----------------|---|
| 0 | 2 | $\frac{3}{2}^+$ | 3.17 | 0.43 | 0 | 1.45 |
| 0.05 | 0 | $\frac{1}{2}^+$ | 1.93 | 0.39 | 0.056 | 3.09 |
| 0.05 | 5 | $11/2^-$ | 0.235 | 0.21 | 0.05 | |
| 0.93 | 4 | $\frac{3}{2}^+$ | 0.276 | 0.19 | 0.90 | 0.381 |
| 1.12 | 2 | $\frac{3}{2}^+$ | 1.03 | 0.065 | 1.11 | 1.47 |
| 1.40 | 2 | $\frac{3}{2}^+$ | 0.477 | 0.029 | 1.37 | 0.802 |
| 1.71 | 2 | $(\frac{3}{2}^+)$ | 0.082 | 0.004 | | |
| 1.91 | (1) | $(\frac{3}{2}^-)$ | 0.125 | 0.007 | | |
| 2.06 | (3) | $(\frac{3}{2}^-)$ | 0.047 | 0.005 | | |
| 2.25 | (2) | $(\frac{5}{2}^+)$ | 0.503 | 0.027 | | |
| 2.45 | (3) | $(\frac{5}{2}^-)$ | 0.234 | 0.021 | | |
| 2.59 | (3) | $(\frac{3}{2}^-)$ | 0.405 | 0.035 | | |
| 2.69 | (3) | $(\frac{5}{2}^-)$ | 2.24 | 0.185 | | |
| 2.93 | | | 0.432 | | | |
| 3.10 | (1) | $(\frac{3}{2}^-)$ | 2.01 | 0.13 | | |
| 3.37 | (1) | $(\frac{3}{2}^-)$ | 1.32 | 0.077 | | |
| 3.51 | (1) | $(\frac{5}{2}^-)$ | 2.44 | 0.15 | | |
| 3.69 | (1) | $(\frac{5}{2}^-)$ | 2.24 | 0.14 | | |
| 3.85 | (1) | $(\frac{3}{2}^-)$ | 0.600 | 0.037 | | |
| 3.93 | (1) | $(\frac{3}{2}^-)$ | 1.53 | 0.095 | | |
| 4.16 | (1) | $(\frac{3}{2}^-)$ | 1.14 | 0.073 | | |
| 4.25 | (1) | $(\frac{3}{2}^-)$ | 0.830 | 0.053 | | |

Bechara et al, Phys Rev C 12 (1975) 1

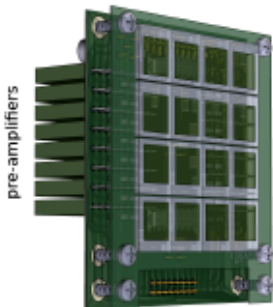
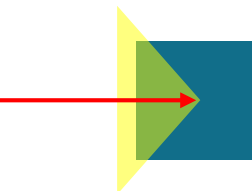


Figure 4: A schematic view of the second detection stage of OSCAR. The rear board contains two series of 8 compact charge sensitive pre-amplifiers to collect signals from 16 silicon pads welded on the front board.



D. Dell'Acqua et al, NIM A 877 (2017) 227

Auxiliary detectors:

- Si Strip Pads (BB7)
- OSCAR-like Si pins
- SPECMAT CeBr3

Challenges:

- High density of states
- Kinematics reconstruction

Summary

Active Targets are promising tools for direct reaction studies, resonant elastic scattering experiments, clustering physics, etc.

BUT

the capabilities of measuring reactions with heavy ions need to be verified
THEREFORE

a better characterization of the ACTAR Demonstrator device is needed.

ACTAR-test aims at

- Getting energy loss information (Shape of the Bragg Peak) to be used for Particle Identification and energy measurement and can be of more general interest [ACTAR Sim, AT-TPC].
 - Using benchmark reactions to validate the techniques.

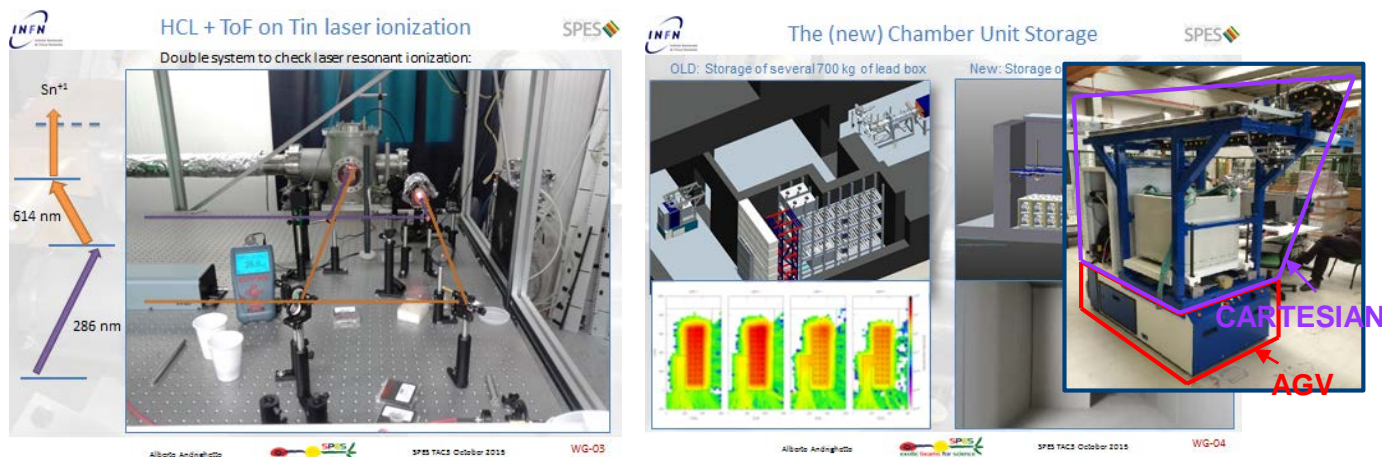
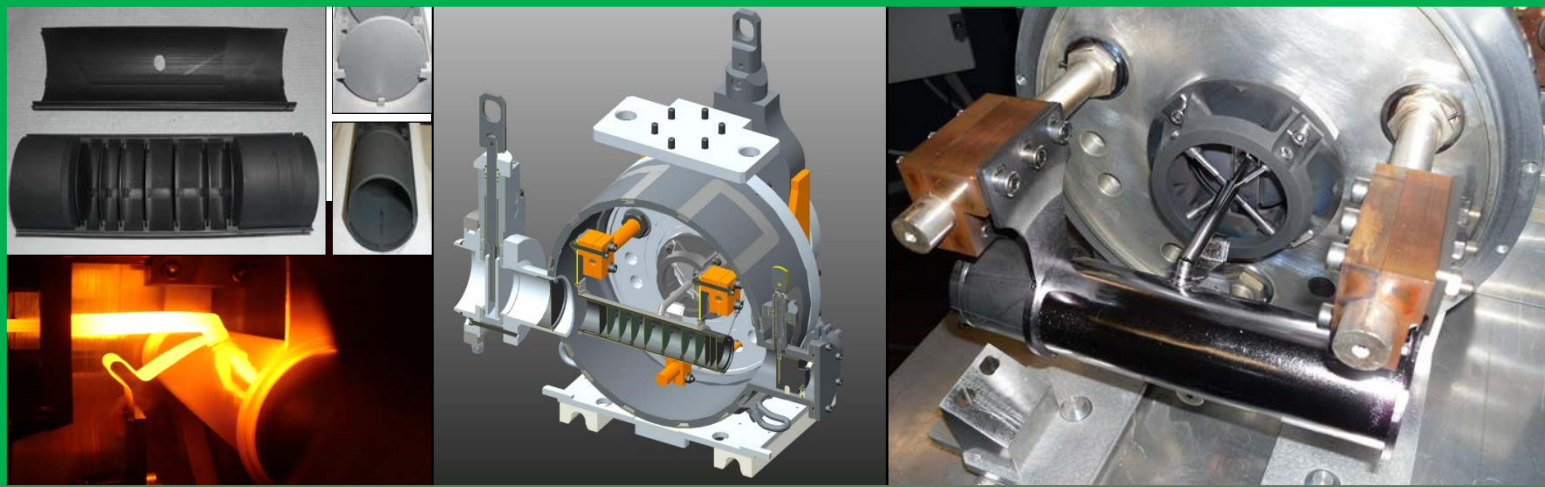
| Test | Topic | Beam | Accelerator | BTU |
|----------|--|---|-------------|-----|
| Part 1 | Energy loss measurements. | Several beams at different energies (see table 1) | Tandem | 45 |
| Part 2-a | $^{19}\text{F}(\text{p},\alpha_0)^{16}\text{O}$ reaction | ^1H at 5.5, 7.0, 8.0 MeV | Tandem | 9 |
| Part 2-b | $^{120}\text{Sn}(\text{d},\text{p})^{121}\text{Sn}$ reaction in inverse kinematics | ^{120}Sn at 15 AMeV | Cyclotron | 21 |

The SPES facility



RIB production: SPES- β

**SPES
ISOL
Target:
UCx, SiC,...
 10^{13} fiss./s
 $T \sim 2000^{\circ}\text{C}$
3 sources SIS,
LIS, PIS
 $\sim 8 \text{ kW}$ power**

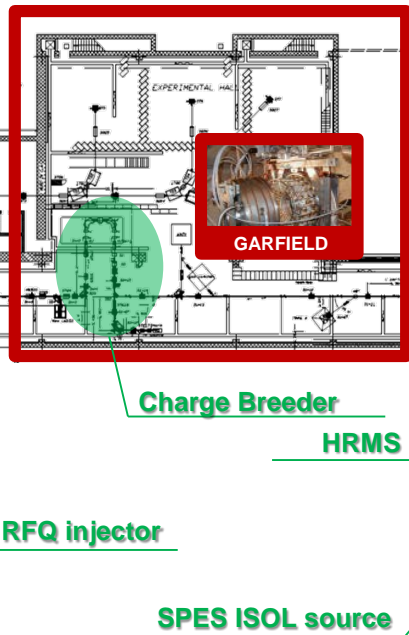
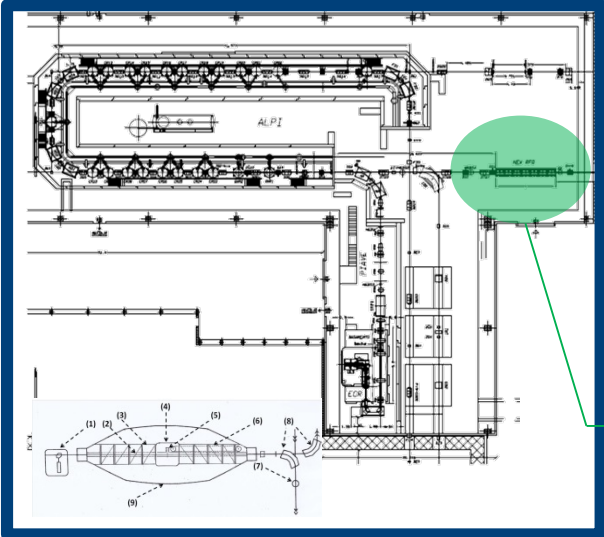


**Beam test at iThemba lab. (2014): 66MeV protons, 60 μA on full scale SiC prototype at 1600 $^{\circ}\text{C}$ (FEM sim. Validation)
Former beam tests: ORNL (2007, 2010-2011) SiC, Ucx; ISOLDE(2009) UCx, IPNO (2013) UCx.**

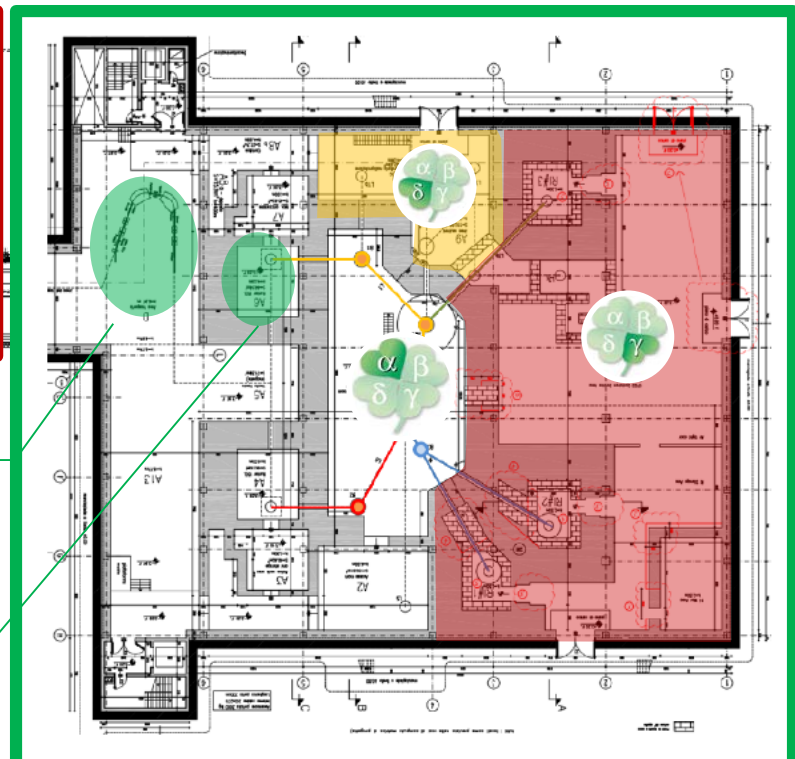
**Front End and Target System: advanced nuclearization phase.
Target handling systems, Heat resistance tests, Nuclear Safety.**

Facility layout

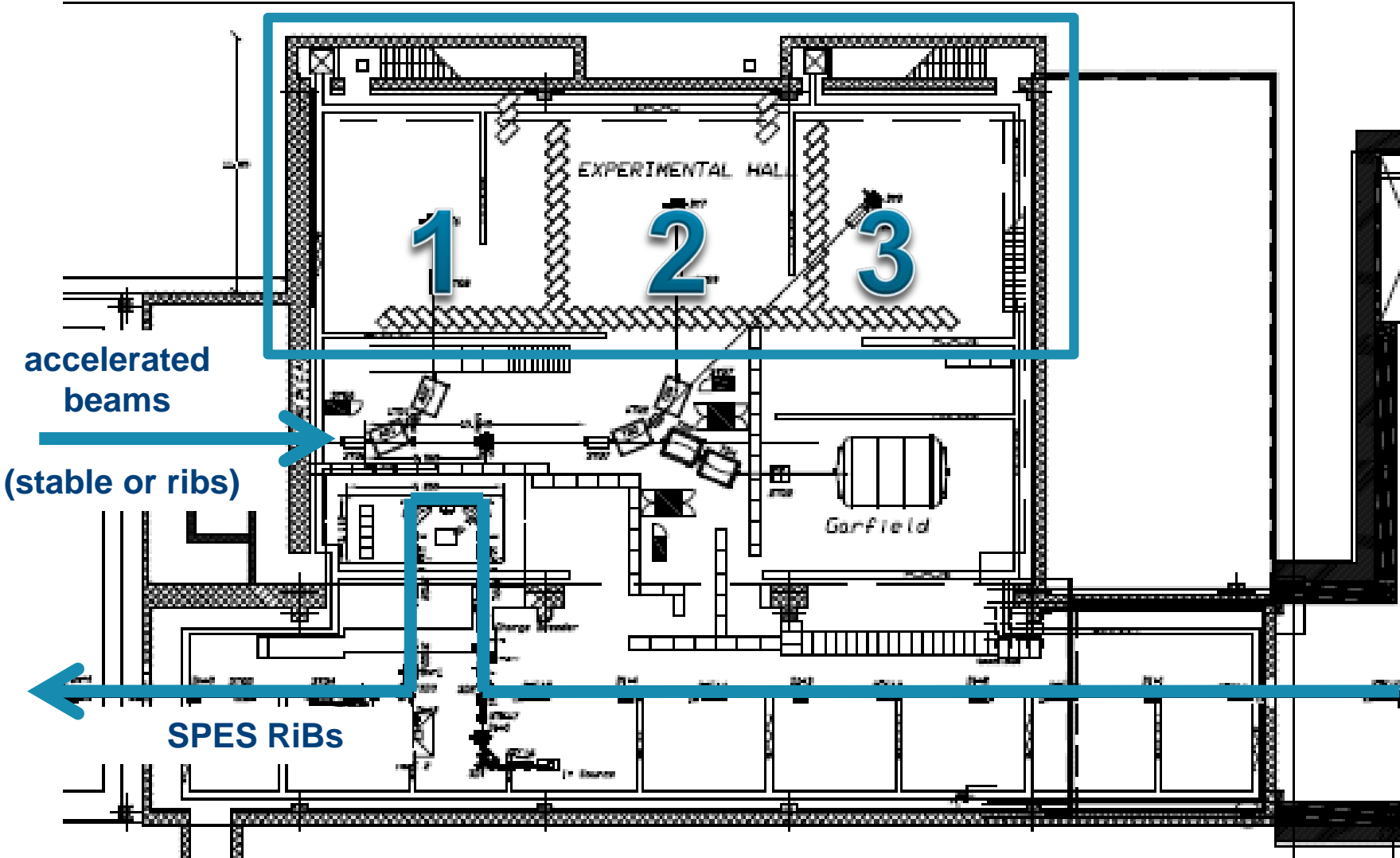
Tandem-Piave-Alpi

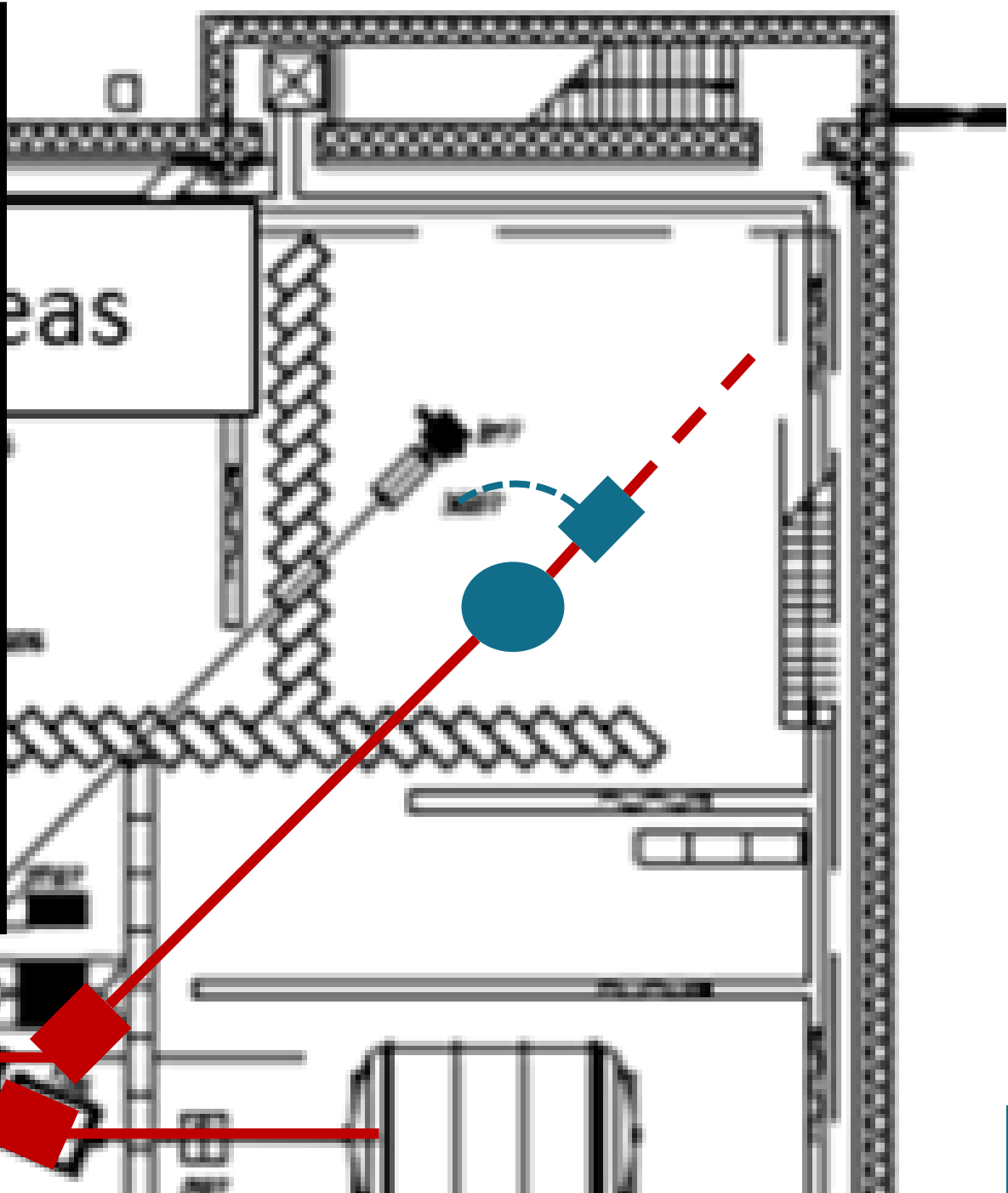
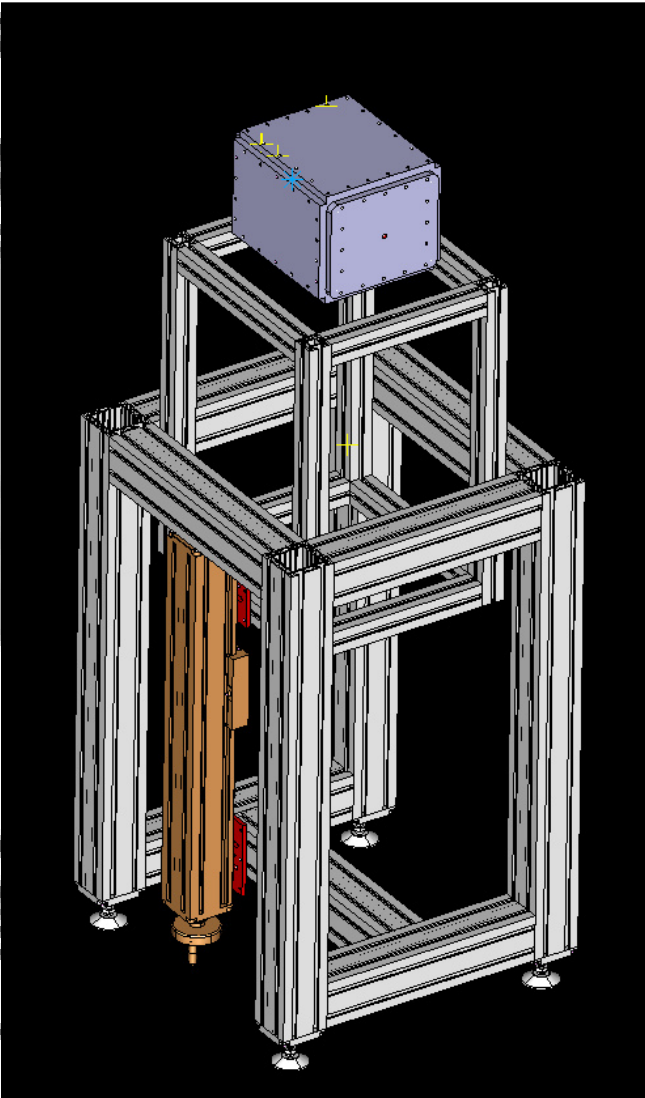


PRISMA GALILEO

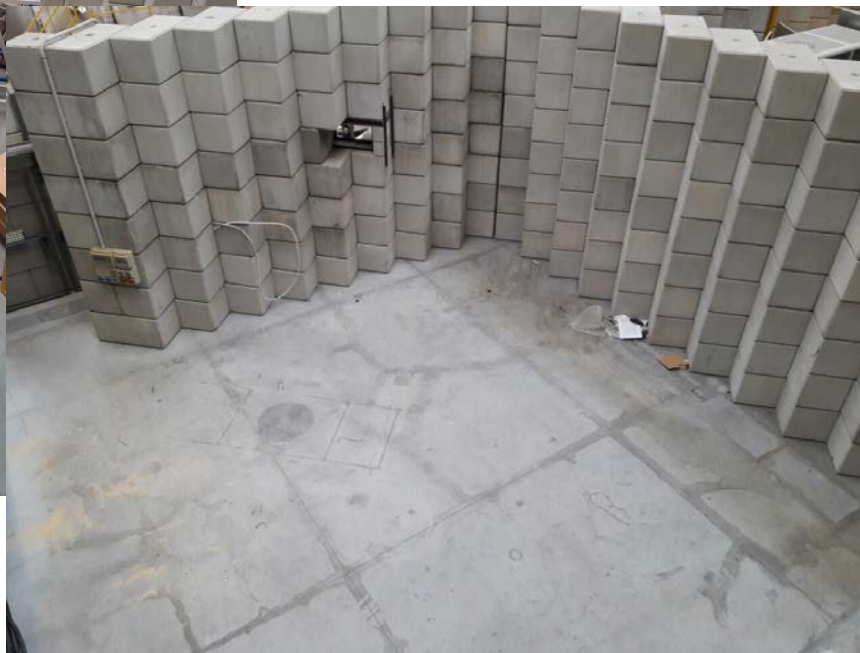


ATS: an Active Target for SPES



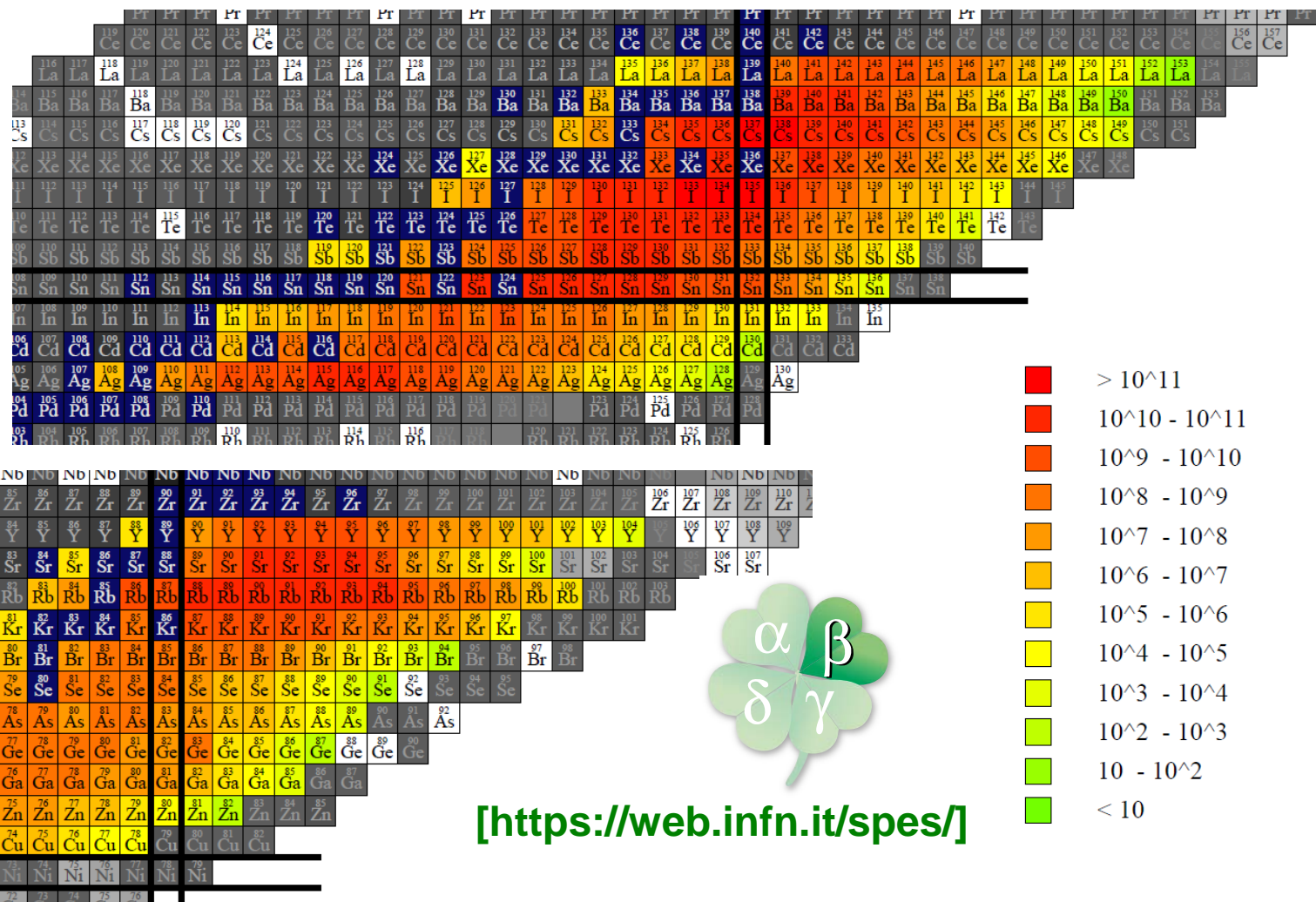






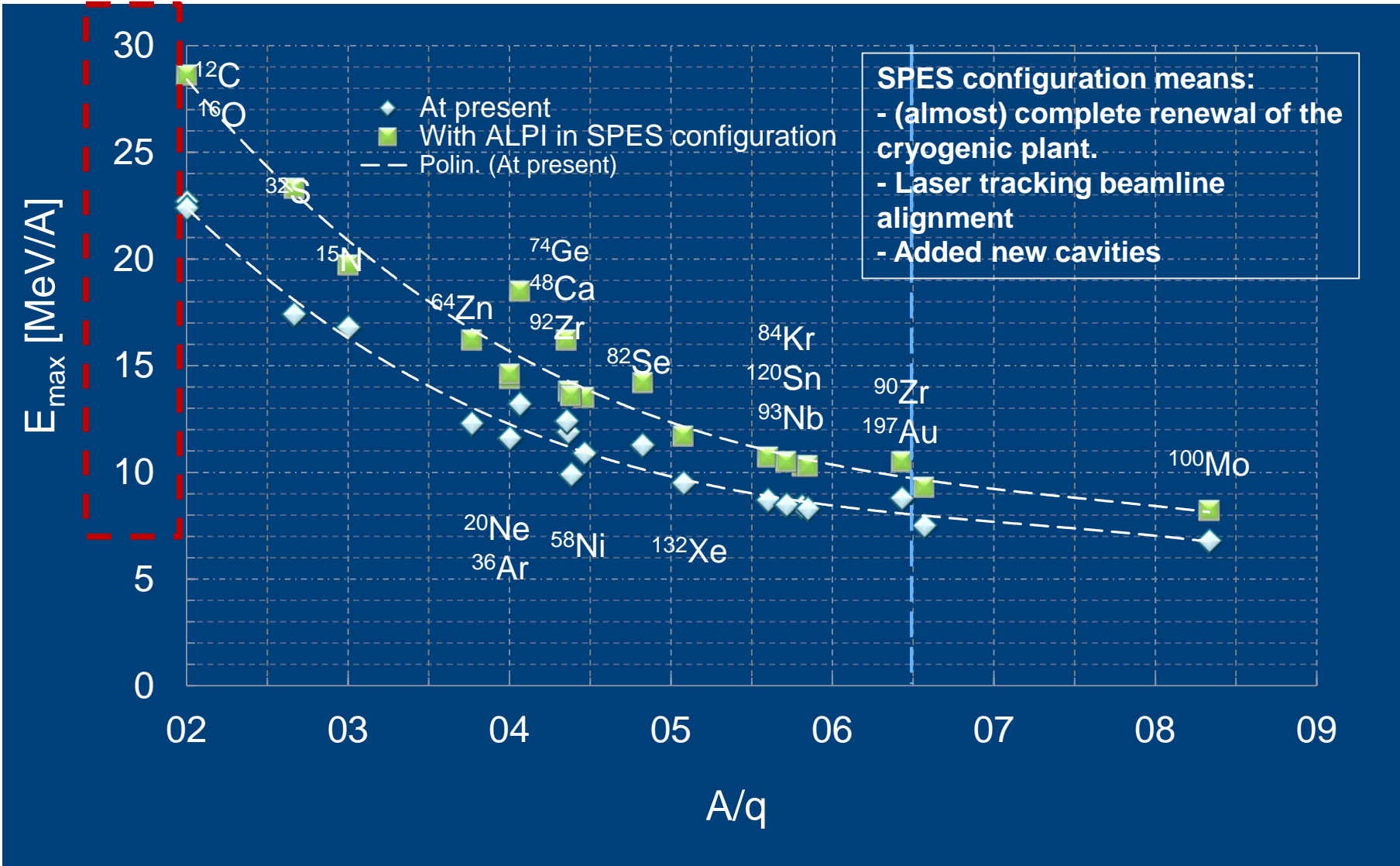


Beyond MagicTin: physics opportunities with an active target at SPES



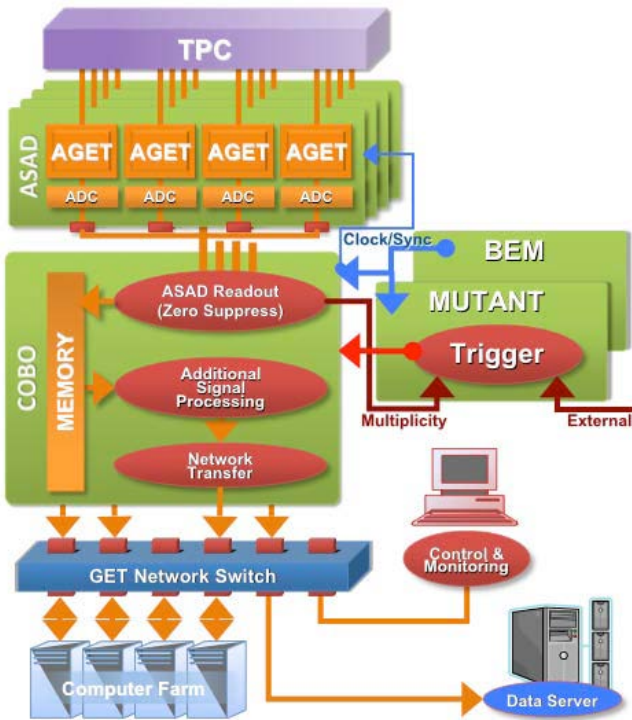
Two letters of intent for SPES endorsed by the SAC:
B. Fernandez Dominguez et al, Direct Reactions with exotic nuclei in the r-process using an active target
R. Raabe, T. Marchi et al, Shell Structure in the vicinity of ^{132}Sn with an active target

Reacceleration using ALPI



GET/GES and GPUs

TPC = 16k ch

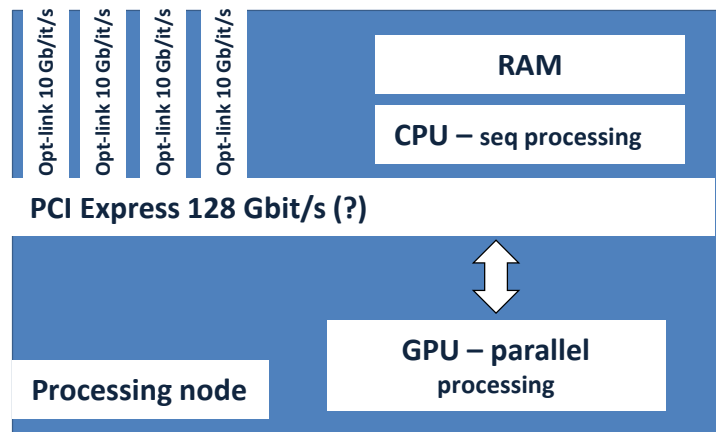


ASAD = 4*AGET + ADC
256 ch →

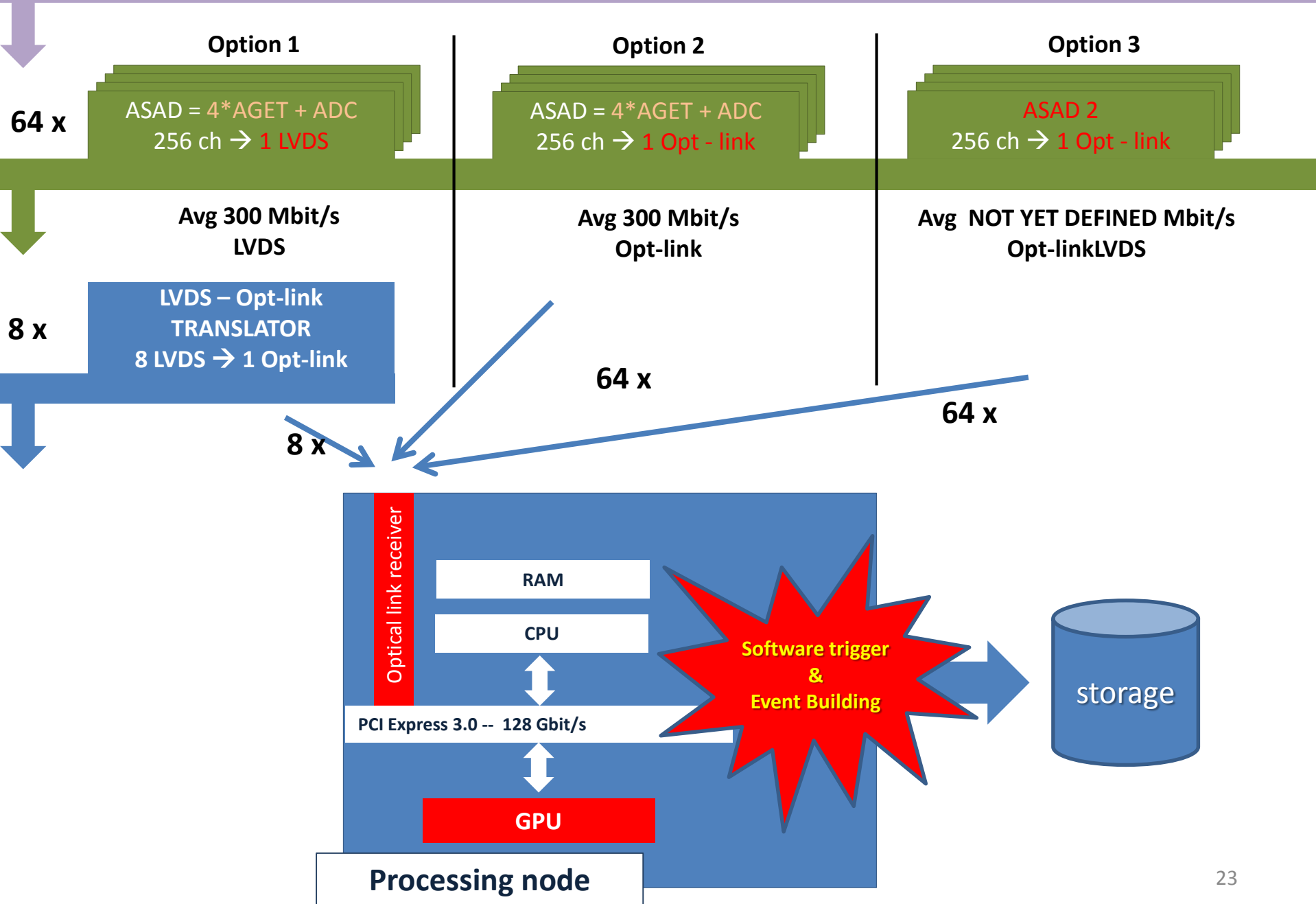
64 x (average) 300 Mbit/s
LVDS standard

NEW DATA
CONCENTRATOR/TRANSLATOR

4 x (average) 10 Gbit/s TCP over
Optical link
-commercial standard and hw-



TPC = 16k ch

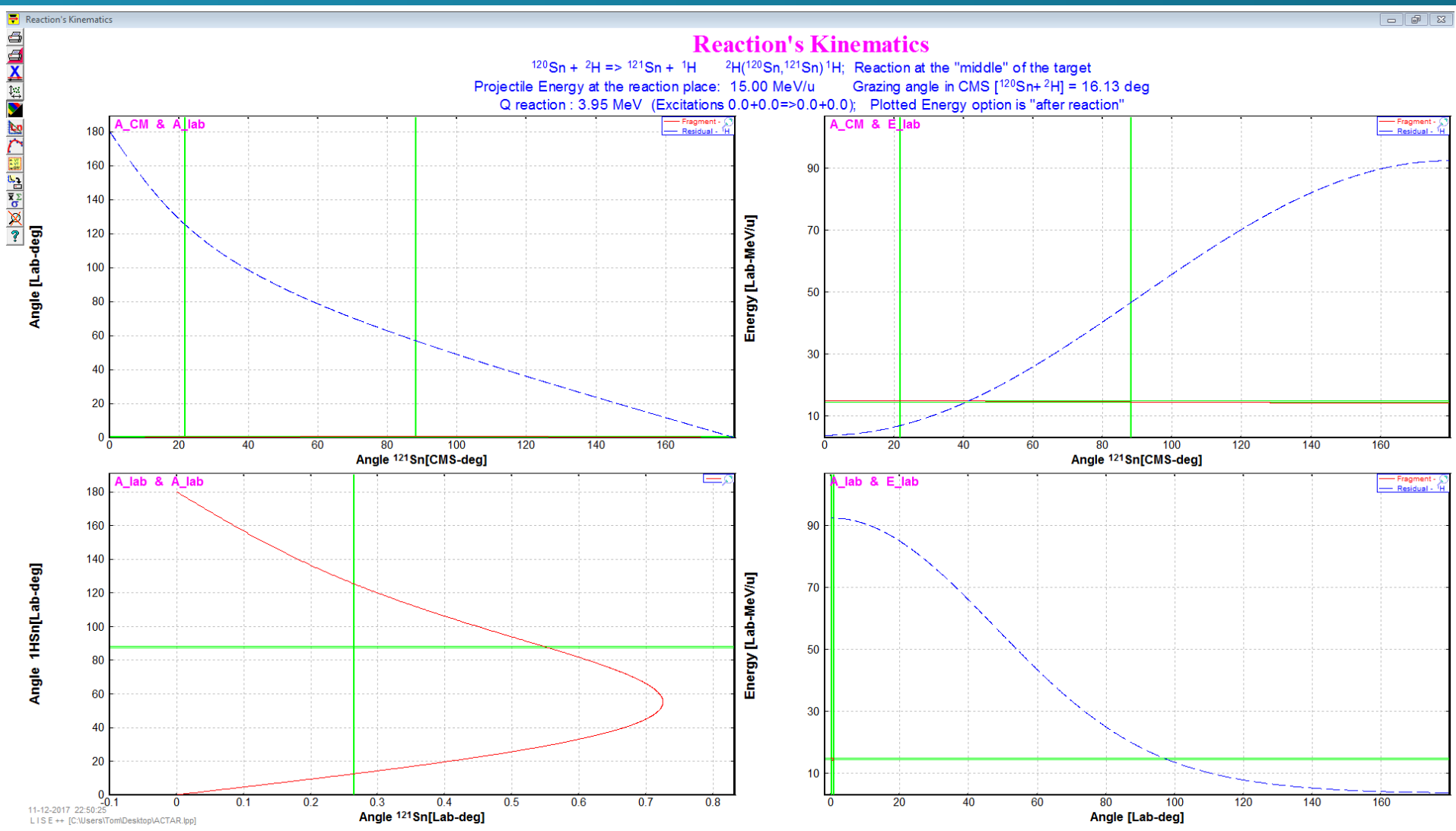




Thank you!

<http://pro.ganil-spiral2.eu/laboratory/detectors/actartpc>

| | iC ₄ H ₁₀ | | | H ₂ | | | CH ₄ | | | CF ₄ | | | CO ₂ | | | D ₂ | | |
|-------------------|---------------------------------|----------|--------------|----------------|-----------|--------------|-----------------|-----------|--------------|-----------------|----------|--------------|-----------------|-----------|--------------|----------------|-----------|--------------|
| BEAM | E/A | PRESSURE | x Bragg Peak | E/A | PRESSURE | x Bragg Peak | E/A | PRESSURE | x Bragg Peak | E/A | PRESSURE | x Bragg Peak | E/A | PRESSURE | x Bragg Peak | E/A | PRESSURE | x Bragg Peak |
| p | 3.5 MeV | 550 mbar | 7.3 cm | 3.5 MeV | 1000 mbar | / | 3.5 MeV | 1000 mbar | / | 3.5 MeV | 550 mbar | 7.2 cm | 3.5 MeV | 1000 mbar | 7.3 cm | 3.5 MeV | 1000 mbar | / |
| d | 1.8 MeV/A | 350 mbar | 7.3 cm | 1.8 MeV/A | 1000 mbar | / | 1.8 MeV/A | 1000 mbar | 9.05 cm | 1.8 MeV/A | 350 mbar | 7.8 cm | 1.8 MeV/A | 650 mbar | 7.5 cm | 1.8 MeV/A | 1000 mbar | / |
| ⁴ He | | | | | | | | | | | | | | | | | | |
| ⁷ Li | 1 MeV/A | 70 mbar | 6.2 cm | 1 MeV/A | 1000 mbar | 4.6 cm | 1 MeV/A | 250 mbar | 5.09 cm | 1 MeV/A | 70 mbar | 7.9 cm | 1 MeV/A | 125 mbar | 7.7 cm | 1 MeV/A | 800 mbar | 7.1 cm |
| ⁹ Be | 1.3 MeV/A | 100 mbar | 4.09 cm | 1.3 MeV/A | 1000 mbar | 6.5 cm | 1.3 MeV/A | 270 mbar | 6.09 cm | 1.3 MeV/A | 100 mbar | 5.4 cm | 1.3 MeV/A | 150 mbar | 7.3 cm | 1.3 MeV/A | 900 mbar | 7.9 cm |
| ¹⁰ B | 1.5 MeV/A | 70 mbar | 7.6 cm | 1.5 MeV/A | 1000 mbar | 6.1 cm | 1.5 MeV/A | 250 mbar | 6.4 cm | 1.5 MeV/A | 80 mbar | 7.2 cm | 1.5 MeV/A | 150 mbar | 7.4 cm | 1.5 MeV/A | 900 mbar | 7.4 cm |
| ¹² C | 1.8 MeV/A | 100 mbar | 5.4 cm | 1.8 MeV/A | 1000 mbar | 7.3 cm | 1.8 MeV/A | 270 mbar | 7.5 cm | 1.8 MeV/A | 100 mbar | 6.3 cm | 1.8 MeV/A | 200 mbar | 5.1 cm | 1.8 MeV/A | 1000 mbar | 8.4 cm |
| ¹⁵ N | 1.8 MeV/A | 100 mbar | 5.4 cm | 1.8 MeV/A | 1000 mbar | 7.3 cm | 1.8 MeV/A | 270 mbar | 7.5 cm | 1.8 MeV/A | 100 mbar | 6.3 cm | 1.8 MeV/A | 200 mbar | 5.1 cm | 1.8 MeV/A | 1000 mbar | 8.3 cm |
| ¹⁶ O | 2 MeV/A | 100 mbar | 5.5 cm | 2 MeV/A | 1000 mbar | 8.6 cm | 2 MeV/A | 270 mbar | 7.7 cm | 2 MeV/A | 100 mbar | 6.5 cm | 2 MeV/A | 200 mbar | 5.3 cm | 2 MeV/A | 1000 mbar | 8.6 cm |
| ¹⁹ F | 1.8 MeV/A | 80 mbar | 6.7 cm | 1.8 MeV/A | 1000 mbar | 6.9 cm | 1.8 MeV/A | 270 mbar | 6.2 cm | 1.8 MeV/A | 100 mbar | 5.3 cm | 1.8 MeV/A | 150 mbar | 7.2 cm | 1.8 MeV/A | 1000 mbar | 6.9 cm |
| ²⁴ Mg | 2 MeV/A | 80 mbar | 6.8 cm | 2 MeV/A | 1000 mbar | 7.09 cm | 2 MeV/A | 250 mbar | 7.2 cm | 2 MeV/A | 100 mbar | 5.6 cm | 2 MeV/A | 125 mbar | 5.8 cm | 2 MeV/A | 1000 mbar | 7.1 cm |
| ⁴⁰ Ca | 2 MeV/A | 80 mbar | 5.6 cm | 2 MeV/A | 1000 mbar | 5.8 cm | 2 MeV/A | 225 mbar | 7.2 cm | 2 MeV/A | 80 mbar | 6.9 cm | 2 MeV/A | 150 mbar | 6.2 cm | 2 MeV/A | 900 mbar | 7.1 cm |
| ¹²⁰ Sn | 1.3 MeV/A | 100 mbar | 5.1 cm | 1.3 MeV/A | 1000 mbar | 7.4 cm | 1.3 MeV/A | 270 mbar | 7.1 cm | 1.3 MeV/A | 100 mbar | 6.9 cm | 1.3 MeV/A | 170 mbar | 7.3 cm | 1.3 MeV/A | 1000 mbar | 7.8 cm |

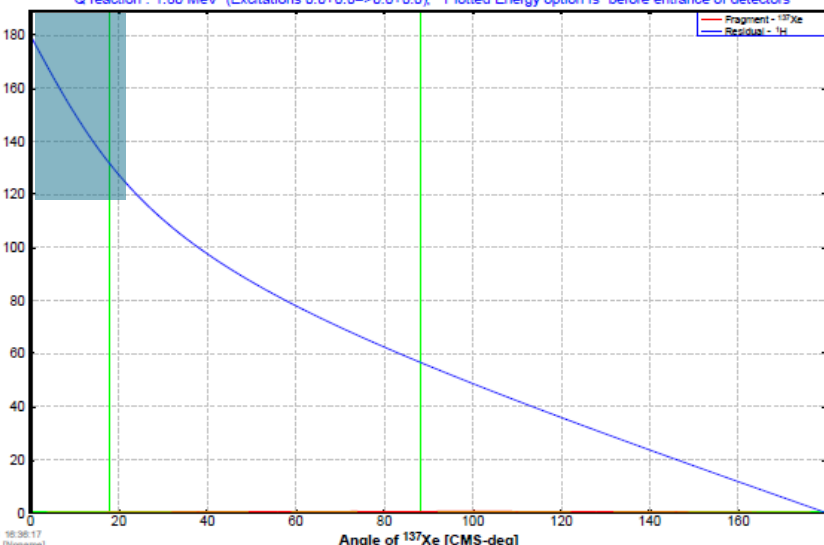


Does kinematics help?

MagicTin*

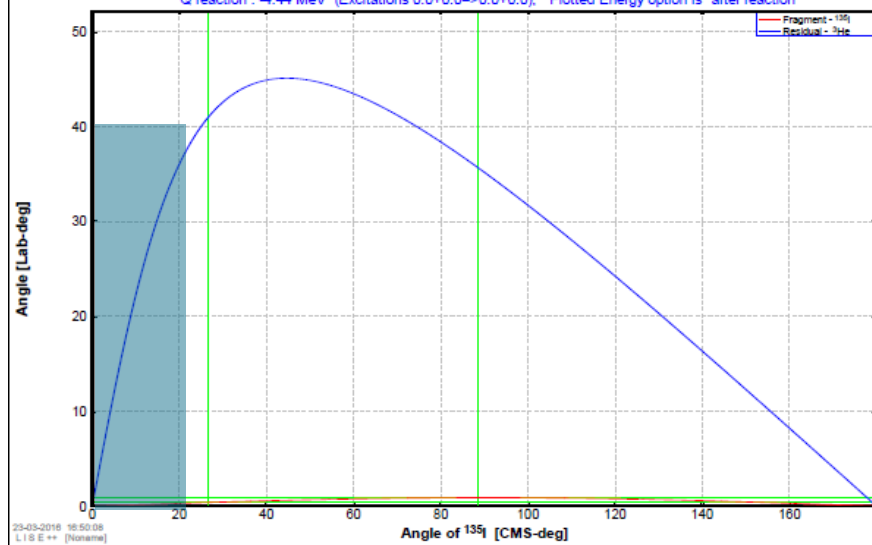
Reaction's Kinematics: A_CM & A_lab

$^{136}\text{Xe} + ^2\text{H} \Rightarrow ^{137}\text{Xe} + ^1\text{H}$ $^2\text{H}(^{136}\text{Xe}, ^{137}\text{Xe})^1\text{H}$; Reaction at the "middle" of the target
 Projectile Energy at the reaction place: 9.97 MeV/u Grazing angle in CMS $[^{136}\text{Xe}+^2\text{H}] = 28.05$ deg
 Q reaction : 1.80 MeV (Excitations 0.0+0.0>0.0+0.0); Plotted Energy option is "before entrance of detectors"

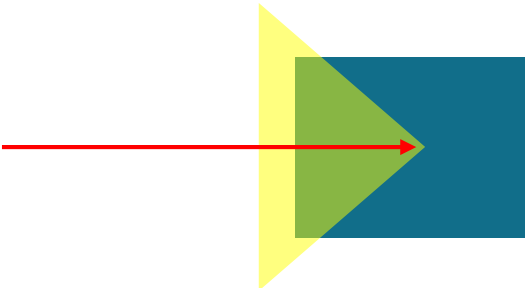


Reaction's Kinematics: A_CM & A_lab

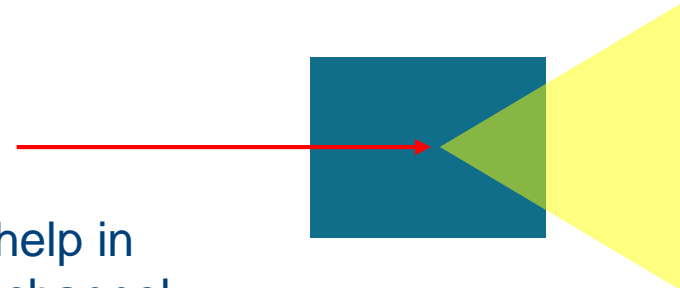
$^{136}\text{Xe} + ^2\text{H} \Rightarrow ^{135}\text{I} + ^3\text{He}$ $^2\text{H}(^{136}\text{Xe}, ^{135}\text{I})^3\text{He}$; Reaction at the "middle" of the target
 Projectile Energy at the reaction place: 9.25 MeV/u Grazing angle in CMS $[^{136}\text{Xe}+^2\text{H}] = 30.87$ deg
 Q reaction : 4.44 MeV (Excitations 0.0+0.0>0.0+0.0); Plotted Energy option is "after reaction"



$^{136}\text{Xe}(d,p)^{137}\text{Xe}$ - inv kinem



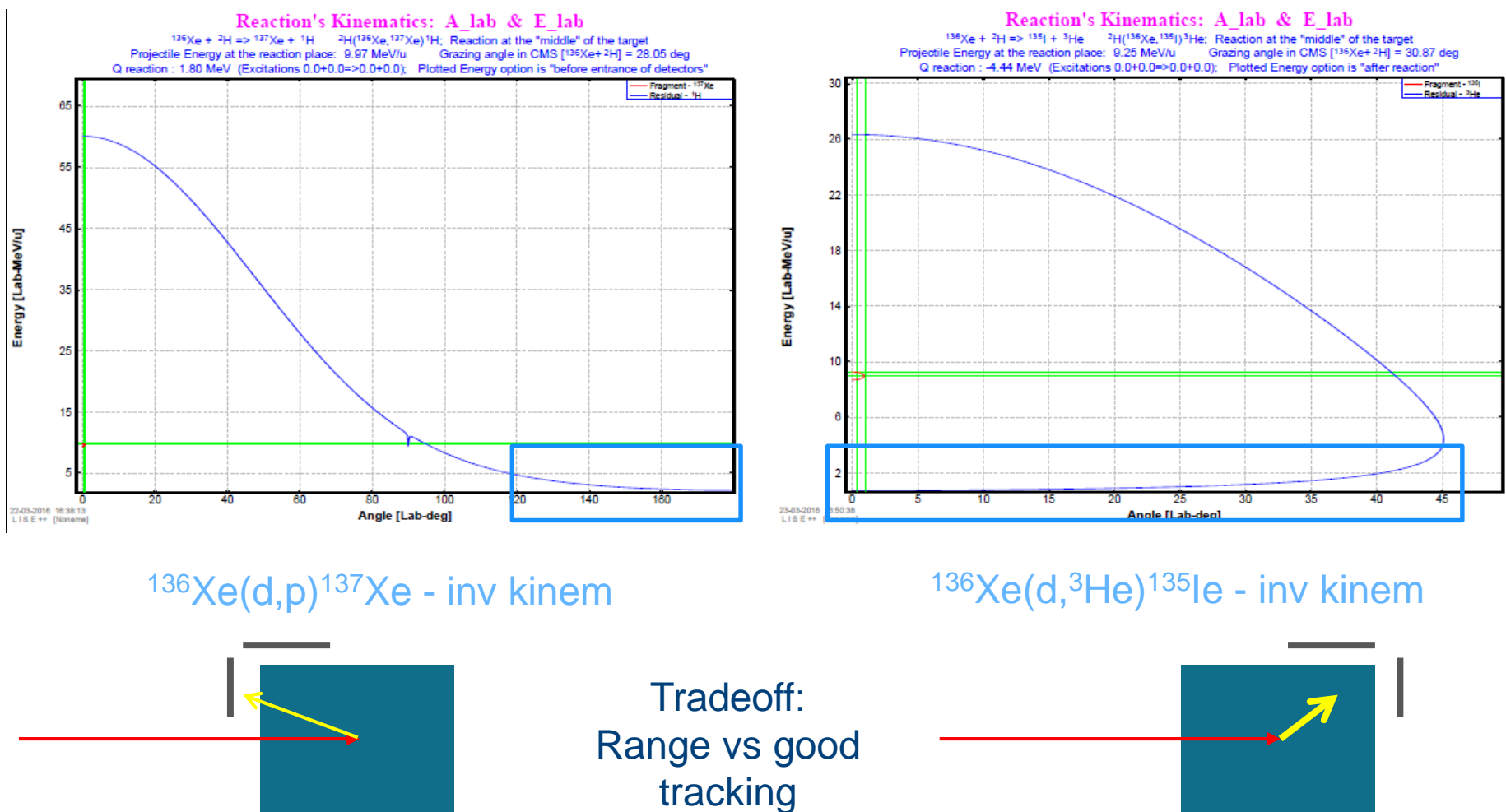
$^{136}\text{Xe}(d,^3\text{He})^{135}\text{I}$ - inv kinem



Kinematics seems to help in selecting the reaction channel

Or not?

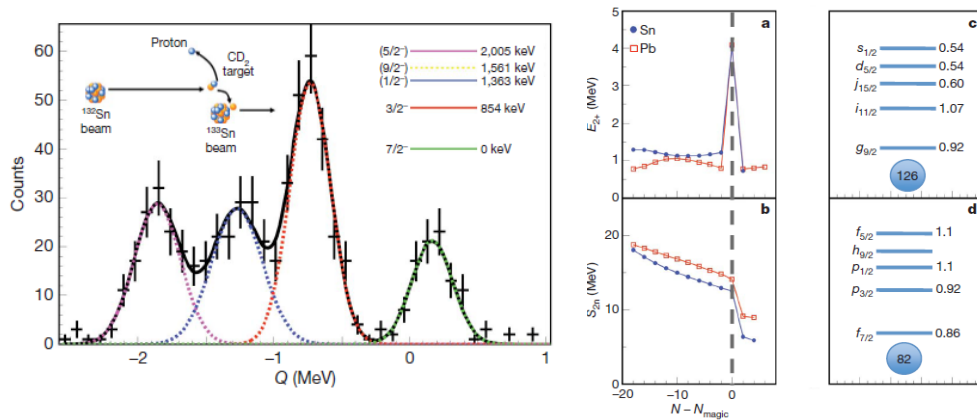
MagicTin*



Getting more details - transfer reactions

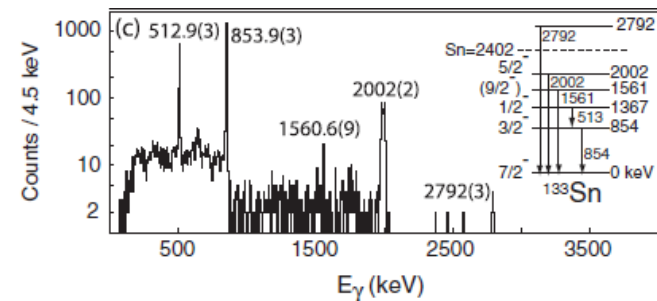
MagicTin[★]

- Probe single particle properties determining spectroscopic factors
- Extend towards more neutron-rich region (+1n)



[K.L. Jones et al, Nature 465 (2010) 454]

Evidences of ^{132}Sn double magicity
Resolution ~ 300 keV



[J.M. Allmond et al, PRL 112, 172701 (2014)]

High resolution spectroscopy for ^{131}Sn ^{133}Sn using (^9Be , ^8Be) transfer reactions

Beyond ^{132}Sn

(11/2-) ————— 3700

(8+) ————— 2508.9

(5/2-) ————— 2004.6

(9/2-) ————— 1560.9

(1/2-) ————— 1363

3/2- ————— 853.7

7/2- ————— 0.0 1.46 S

^{133}Sn

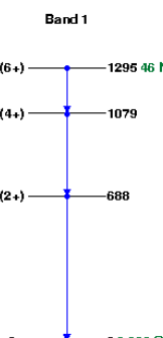
$d(^{132}\text{Sn}, ^{133}\text{Sn})p$
Q = 177 keV

^{134}Sn

$d(^{133}\text{Sn}, ^{134}\text{Sn})p$
 $Q_{\text{gs}} = 1.4 \text{ MeV}$

^{135}Sn

$d(^{134}\text{Sn}, ^{135}\text{Sn})p$
Q = 47 keV

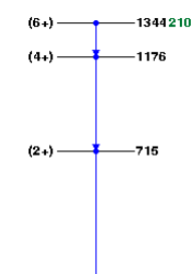


^{136}Sn

$d(^{135}\text{Sn}, ^{136}\text{Sn})p$
Q = 1.1 MeV

^{137}Sn
0 190 MS

$d(^{136}\text{Sn}, ^{137}\text{Sn})p$
Q = -264 keV



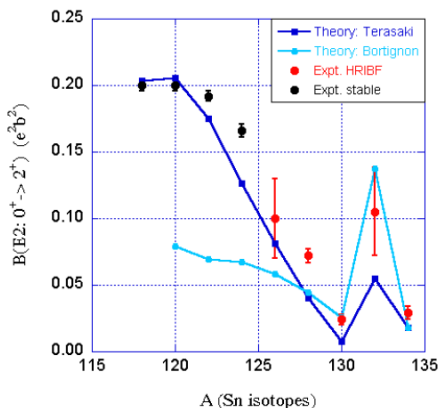
^{138}Sn

$d(^{137}\text{Sn}, ^{138}\text{Sn})p$
Q = 0.9 MeV

Expected beam intensities @ 10 AMeV

| | SPES 1 st day (5 μA p beam) | SPES full power (200 μA p beam) |
|-------------------|--|---|
| ^{132}Sn | 7.8 10⁵ | 3.1 10⁷ |
| ^{133}Sn | 7.0 10⁴ | 2.8 10⁶ |
| ^{134}Sn | 1.2 10⁴ | 4.9 10⁵ |
| ^{135}Sn | 1.6 10² | 6.2 10³ |
| ^{136}Sn | - | 0.9 10² |

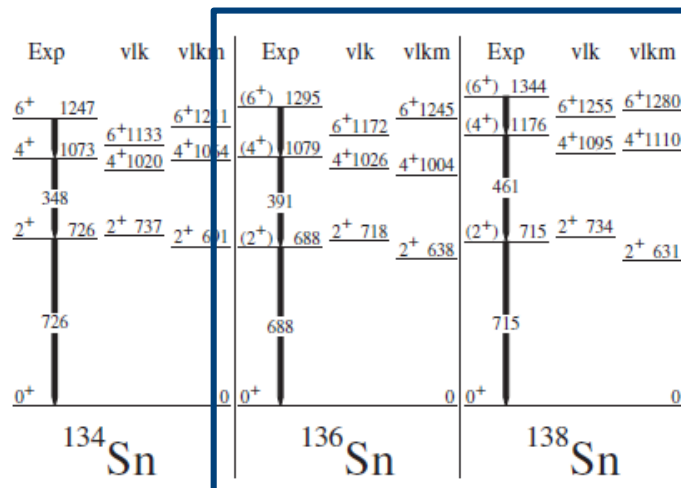
Shell evolution and collectivity in Tin isotopes



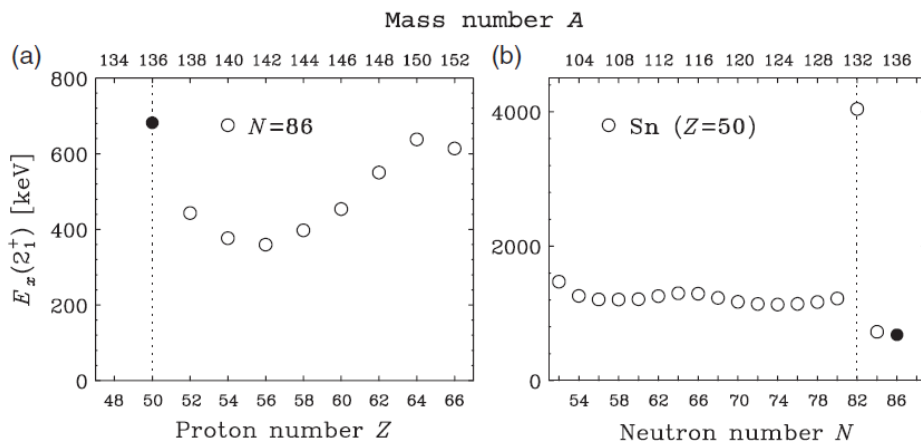
[R.L. Varner et al, EPJA 25 (2005) 391]

132,134Sn Coulex @ HRIBF
9000 ions/s
150 BaF₂ (~30% eff)

9Be(137Sb, 136Sn) @ RIKEN DALI2 (186 NaI(Tl) ~22% eff)



[G. Simpson et al, Phys Rev Lett 113 (2014) 132502]



[He Wang et al, PTEP 023D02 (2014)]

RIBF 238U
345 MeV/u